International Journal of Engineering, Mathematical and Physical Sciences
ISSN: 2517-9934
Vol:14, No:12, 2020

Dual-Actuated Vibration Isolation Technology for a Rotary System's Position Control on a Vibrating Frame: Disturbance Rejection and Active Damping

Kamand Bagherian, Nariman Niknejad

***Abstract*—A vibration isolation technology for precise position control of a rotary system powered by two permanent magnet DC (PMDC) motors is proposed, where this system is mounted on an oscillatory frame. To achieve vibration isolation for this system, active damping and disturbance rejection (ADDR) technology is presented which introduces a cooperation of a main and an auxiliary PMDC, controlled by discrete-time sliding mode control (DTSMC) based schemes. The controller of the main actuator tracks a desired position and the auxiliary actuator simultaneously isolates the induced vibration, as its controller follows a torque trend. To determine this torque trend, a combination of two algorithms is introduced by the ADDR technology. The first torque-trend producing algorithm rejects the disturbance by counteracting the perturbation, estimated using a model-based observer. The second torque trend applies active variable damping to minimize the oscillation of the output shaft. In this practice, the presented technology is implemented on a rotary system with a pendulum attached, mounted on a linear actuator simulating an oscillation-transmitting structure. In addition, the obtained results illustrate the functionality of the proposed technology.**

***Keywords*—Vibration isolation, position control, discrete-time nonlinear controller, active damping, disturbance tracking algorithm, oscillation transmitting support, stability robustness.**

I. Introduction

IN current industrial applications, rotating electrical machines, including AC or DC motors, are commonly installed on moving or vibrating structures. Vibratory forces resulted from the oscillation of these structures are often inevitable, and in such scenarios, precise motion control of these machines becomes challenging, as the transmitted excessive vibration to the system, from its structure, imposes disturbance on the output shaft of the electrical machine. Thus, a proper vibration isolator is required to minimize these detrimental effects on the dynamical system. Vibration isolation methods are classified into two major categories, passive and active [1]. The passive method equips a system with auxiliary mechanical devices such as springs and dampers, to absorb the undesired effect of the imposed force [2], [3] and the active method, utilizes a suitable control scheme, sensors, and an auxiliary actuator to cancel the disturbance caused by the oscillation. Despite the ease of implementation of the passive method, active vibration isolation is more flexible, as the control parameters can be regulated based on the needs of each application. Thus, the active scheme has a better performance in comparison to the passive. In the available literature, active vibration isolation methods have been applied to rotating machinery mostly using direct active vibration control techniques. These techniques are done by applying a lateral control force to the rotor, which is generated by a force actuator, such as a magnetic bearing [4]–[7], however, the available vibration control techniques cannot suppress vibration in the same direction the position of a rotary actuator needs to be controlled, meaning rotational vibration suppression. Moreover, active magnetic bearings are costly, have reliability problems, and the robustness of their control algorithms is still an important issue. In articles such as [8], Knospe et al. examined how implementing an adaptive controller improves the robustness of vibration control using active magnetic bearings. However, adaptive controllers increase the order of the system's dynamics, leading to a more complex dynamic model and an undesirable increase in computational time. Besides, these controllers are designed in continuous time and are not easily discretized for digital implementations. Another approach for having a more precise position control of rotary configurations in the presence of vibration is to consider an estimation of the disturbance by deploying an observer, in the dynamic model of the system [9]. In [10], Shanaka et al. proposed an active vibration suppression system, using a force observer to reduce the induced radial vibration, without an auxiliary actuator. Nevertheless, in PMDC motors, the differential equation between current and voltage is first-order, and third-order between position and voltage. Therefore current (torque) control has a faster response compared to position control. That is to say, torque control would have a better and faster performance for disturbance rejection, in comparison with position control. Due to the presence of disturbance on the output shaft, the position controller fails to reach its desired position, and the controller needs additional time to minimize the caused error [11]. As a result, if a system is mounted on a vibrating or moving frame, assistive torque control is needed for an effective disturbance rejection to suppress the deteriorating vibrational effect. To achieve a more efficient disturbance rejection, a robust nonlinear model-based controller is required. Such controllers are relatively superior in performance, as the dynamics of the system, modeling uncertainty, and imposed loads can be fully considered. The sliding mode control method is a nonlinear model-based control scheme. Furthermore, this controller is easily discretized and effortlessly implemented on digital

Kamand Bagherian and Nariman Niknejad* are with the Department of Mechanical Engineering, K. N. Toosi University of Technology, Tehran, Iran (*corresponding author, phone: +989372280651, e-mail: nzn0031@auburn.edu)

devices, as opposed to continuous-time based controllers [12]. Therefore, DTSMC is one of the most-used methods to deal with the previously mentioned difficulties. I n t his a rticle, a new technology for vibration isolation is proposed to improve tracking precision and performance quality in the presence of external disturbances caused by undesired vibrational effects. The proposed ADDR technology involves the cooperation of two actuators: a main actuator responsible for position control and an auxiliary actuator utilized for vibration isolation. This consists of disturbance rejection and active variable damping. An observer is introduced to estimate the value of the disturbance without further need of calculation to operate in different situations. DTSMC is utilized as the control method to track both the desired position and torque (armature current) trends. The stability of the controllers is guaranteed using Lyapunov-based calculations, and the performance of the ADDR technology is evaluated using real-time experiments, by implementation on an experimental setup consisting of a dual-actuated rotary system mounted on a linear actuator. The linear actuator tracks a trajectory to simulate a high-amplitude and low-frequency motion of moving/vibrating industrial structures. Two coupled PMDC motors, working in series and connected by belt and pulley configuration, f orm the dual-actuated rotary system. A load-carrying pendulum is attached to the common output shaft of the dual-actuated rotary system. The energy loss of this configuration is negligible. This design is energy and cost-efficient s ince all the necessary parts are integrated into a single configuration. This article is arranged as follows: Section II presents the model of the ADDR machine, and in Section III the DTSMC-based controllers for this machine are developed. The proposed ADDR method is introduced in Section IV that is designed to isolate the system from the exerted vibrational effects. Section V illustrates the evaluation of the proposed technology by experimental results.

II. Model of the ADDR Machine

A. Model of the Dual-Actuated Rotary System

This section presents the mathematical modeling procedure of the ADDR machine, which is a dual-actuated rotary system, mounted on a moving and vibrating cart, causing a disturbance in the system. The general configuration of the rotary-actuated system is shown in Fig. 1. The two PMDC motors transmit power to the load-carrying pendulum using pulleys and a belt.

The mathematical model of the system, considering the unknown disturbance, is derived as (1):

$$J_{eq}\ddot{\theta} = \tau_t - mglsin\theta + \tau_d \tag{1}$$

where τ_t is the total generated torque of the actuators $(N.m)$, τ_d is the disturbance of the system $(N.m)$, J_{eq} is the effective mass moment of inertia of the rotation axis $(kg.m^2)$, m is the mass of the pendulum (kg), l is the length of the pendulum, g is the gravitational acceleration $(\frac{m}{s^2})$, $\theta\,(rad)$ and $\ddot{\theta}$ $(\frac{rad}{s^2})$ are the angular position and angular acceleration of the actuator's common output shaft, respectively.

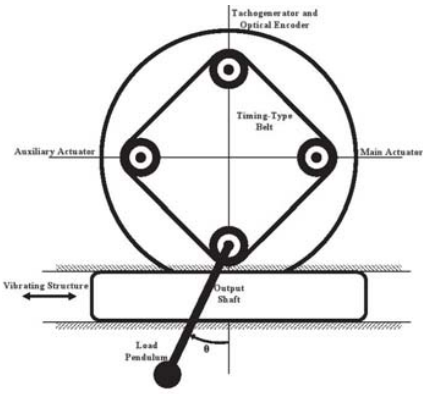

Fig. 1 The free body diagram of the dual-actuated rotary system

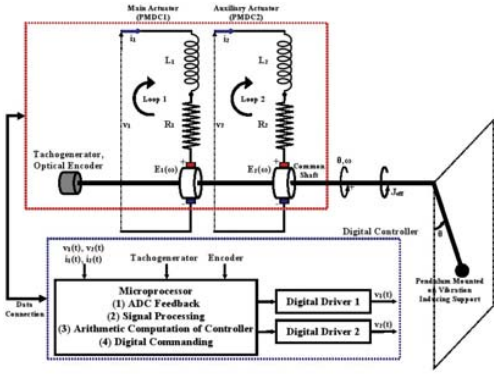

Fig. 2 Electrical diagram of the ADDR machine

The dynamics of the cart is not considered in this mathematical model, as its motion is assumed to be a simulation of a moving and vibrating system structure, producing the main proportion of disturbance in the system.

B. Motor Dynamics

As mentioned, two PMDC motors are used for the technology proposed in this article; a main and an auxiliary PMDC. Fig. 2 represents the schematic overview of the equivalent electrical circuit of the ADDR machine. Equation (2) is the mathematical model of the proposed ADDR machine [13].

$$\begin{cases} \frac{di_1}{dt} = -\frac{R_1}{L_1}i_1 - \frac{K_{e1}}{L_1}\dot{\theta} + \frac{1}{L_1}v_1 \\ \frac{di_2}{dt} = -\frac{R_2}{L_2}i_2 - \frac{K_{e2}}{L_2}\dot{\theta} + \frac{1}{L_2}v_2 \\ J_{eq}\frac{dw}{dt} = \tau_t - mglsin\theta + \tau_d \\ \tau_t = K_{t1}i_1 + K_{t2}i_2 \\ \frac{d\theta}{dt} = \omega \end{cases} \tag{2}$$

In all the indices, 1 and 2 refer to the characteristics of the main and auxiliary PMDC actuators respectively, where i_1 and i_2 are the currents, v_1 and v_2 show the input voltages; L_1 and L_2 are the electric inductance , R_1 and R_2 represent the winding resistances, K_{e1} and K_{e2} are the back-EMF constants, K_{t1} and K_{t2} are the torque constants. ω $(\frac{rad}{s})$ is the angular velocity of the common output shaft.

Assumption set

1) Back-EMF and torque coefficients (K_e and K_t respectively) are assumed to be constant.
2) The two PMDC machines are identical. ($K_{t1} = K_{t2}, K_{e1} = K_{e2}, L_1 = L_2, R_1 = R_2$)
3) Any mechanical disturbance is assumed to be included in the term τ_d, and it is not directly measurable.
4) The effects of temperature on the PMDC parameters are negligible.

III. Control Development for the ADDR Machine

A. Control Objectives

- The system should be asymptotically stable in the presence of modeling uncertainty.
- The control system should be designed to be stable in discrete-time for digital implementation practices.
- Position tracking should have an acceptable precision in the presence of severe disturbance caused by detrimental vibrations of its structure.
- Two control schemes should be developed to achieve the ADDR technology, a position controller for the main actuator, and a torque controller for active variable damping and disturbance rejection purposes using the auxiliary actuator.

B. Discretization of the ADDR System Model

To accomplish the control objectives stated in part A of section III, the DTSMC method is developed for position control, thus the preceding set of equations (2) is discretized [14] and presented below.
According to Assumption 2:

$$R \triangleq R_2, L \triangleq L_1 = L_2, K_e \triangleq K_{e1} = K_{e2}, K_t \triangleq K_{t1} = K_{t2}$$

$$\begin{cases} i_1(k) = i_1(k-1) + \frac{3T}{2}[i_1(k-1) + a_{12}\omega(k-1) \\ +b_1 v_1(k-1)] - \frac{T}{2}[a_{11} i_1(k-2) + a_{12}\omega(k-2) \\ +b_1 v_1(k-2)] \\ \\ i_2(k) = i_2(k-1) + \frac{3T}{2}[i_2(k-1) + a_{12}\omega(k-1) \\ +b_2 v_2(k-1)] - \frac{T}{2}[a_{11} i_2(k-2) + a_{12}\omega(k-2) \\ +b_2 v_2(k-2)] \\ \\ i(k) = i_1(k) + i_2(k) \\ \\ \omega(k) = \omega(k-1) + \frac{3T}{2}\big[a_{21} i(k-1) + a_{22}[sin\theta(k-1)]\big] \\ -\frac{T}{2}\big[a_{21} i(k-2) + a_{22}[sin\theta(k-1)]\big] + \tau_d^*(k-1) \\ \\ \theta(k) = \theta(k-1) + \frac{3T}{2}\omega(k-1) - \frac{T}{2}\omega(k-2) \end{cases} \tag{3}$$

$$\begin{cases} \phi \triangleq \{R_1, R_2, L_1, L_2, K_{e1}, K_{e2}, K_{t1}, K_{t2}, J_{eq}\}, \phi \subseteq \phi_U \\ a_{11} = -\frac{R}{L}, a_{12} = -\frac{K_e}{L}, a_{21} = K_t/J_{eq}, a_{22} = -\frac{mgl}{J_{eq}} \\ b_1 = \frac{1}{L}, \tau_d^* = \frac{3T}{2}\frac{1}{J}\tau_d(k-1) - \frac{T}{2}\frac{1}{J}\tau_d(k-2) \end{cases}$$

In this set of equations, ϕ is the system's parameters vector, and U is the uncertainty space over which the parameters are defined. As a result of discretization, the time step is defined as $T(s)$.

C. DTSMC-Based Position Controller

For the objective of position control of the ADDR machine, the sliding surface is defined (4).

$$s_1(k) \triangleq \tilde{\theta}(k+1) + \lambda_1 \tilde{\theta}(k), \tilde{\theta}(k) \triangleq \theta(k) - \theta_d(k), |\lambda_1| < 1 \tag{4}$$

where θ_d(k) is the desired angular position and $s_1(k)$ is the sliding surface for position control. A Lyapunov function, denoted by $V_1(k)$, is defined in discrete-time and the inequality $V_1(k+1) - V_1(k) < 0$ is solved along the dynamics of the system and presented in (5) and (6):

$$V_1(k) \triangleq {s_1}^2(k), V_1(k+1) - V_1(k) < 0 \tag{5}$$

$${s_1}^2(k+1) - {s_1}^2(k) < 0 \rightarrow |s_1(k+1)| < |s_1(k)| \tag{6}$$

and from (4), $s_1(k+1)$ is one step ahead of $s_1(k)$:

$$\begin{cases} s_1(k+1) = \xi_1[\underline{x}(k), \phi] + \frac{T}{2}(5 + 3\lambda_1)\tau_d^*(k-1) \\ -\frac{3T}{2}\tau_d^*(k) + \frac{27T^3}{8} a_{21} b_1 v_1(k-1) \end{cases} \tag{7}$$

$$\begin{cases} \xi_1[\underline{x}(k), \phi] = (1+\lambda_1)[\theta(k-1) + \frac{3T}{2}\omega(k-1) \\ -\frac{T}{2}\omega(k-2)] + \frac{T}{2}(5+3\lambda_1)\Big[\omega(k-1) + \frac{3T}{2}\big[a_{21} i(k-1) \\ +a_{22} sin[\theta(k-1)]\big] - \frac{T}{2}\big[a_{21} i(k-2) + a_{22} sin[\theta(k-2)]\big]\Big] \\ -\frac{T}{2}\omega(k-1) + \frac{9T^2}{4}\Big[a_{21}\big[i(k-1) + \frac{3T}{2}[a_{11} i(k-1) \\ +a_{12}\omega(k-1)] - \frac{T}{2}[a_{11} i(k-2) + a_{12}\omega(k-2) \\ +b_1 v_1(k-2)]\big] + a_{22} sin[\theta(k-1) + \frac{3T}{2}\omega(k-1) \\ -\frac{T}{2}\omega(k-2)]\Big] - \frac{3T^2}{4}\big[a_{21} i(k-1) + a_{22} sin[\theta(k-1)]\big] \\ -\lambda_1 \frac{T}{2}\omega(k-1) - \theta_d(k+2) - \lambda_1 \theta_d(k+1) \end{cases} \tag{8}$$

where $\underline{x}(k)$ is the state vector as presented in (9).

$$\begin{cases} \underline{x}(k) \triangleq [v_1(k-2), v_2(k-2), i_1(k-1), i_1(k-2), \\ i_2(k-1), i_2(k-2), \omega(k-1), \omega(k-2)]^T \\ , \underline{x}(k) \in \mathbb{R}^{(8\times 1)} \end{cases} \tag{9}$$

The following $sup(.)$ and $inf(.)$ operators limit the upper and lower bounds of the stable region for the input voltage, computed over the uncertainty space ϕ_U [6]. The variables of these operators are symbolic and converted to numerical values for digital implementation purposes.

$$\begin{cases} \frac{1}{min(b_1)}\frac{2}{3T} sup\big[-\xi_1[\underline{x}(k), \phi] - |s_1(k)|\big]_{\phi_U} < v_1(k-1) \\ < \frac{1}{max(b_1)}\frac{2}{3T} inf\big[-\xi_1[\underline{x}(k), \phi] + |s_1(k)|\big]_{\phi_U} \end{cases} \tag{10}$$

The $sup(.)$ and $inf(.)$ operators that are mentioned in this equation, narrow the stability region, resulting in a a robust controller.

$$\begin{cases} v_1(k-1) = (1-\alpha_1)\Big[\frac{1}{max(b_1)}\frac{2}{3T} inf\big[-\xi_1[\underline{x}(k), \phi] \\ +|s_1(k)|\big]_{\phi_U}\Big] + \alpha_1\Big[\frac{1}{min(b_1)}\frac{2}{3T} sup\big[-\xi_1[\underline{x}, \phi] \\ -|s_1(k)|\big]_{\phi_U}\Big], 0 \le \alpha_1 \le 1 \end{cases} \tag{11}$$

D. DTSMC-Based Torque Controller

For vibration isolation using the auxiliary actuator, a sliding surface for torque (armature current) control is required. Similar to the development of the position controller, it is designed in discrete-time and presented in (12).

$$s_2(k) \triangleq \tilde{i}_2(k-1)+\lambda_2\tilde{i}_2(k-2), \tilde{i}_2(k) \triangleq i_2(k)-i_d(k), |\lambda_2| < 1 \quad (12)$$

Another Lyapunov function, denoted by $V_2(k)$, is defined in discrete-time and the inequality $V_2(k+1)-V_2(k) < 0$ is solved along the dynamics of the system and presented in (13) and (14).

$$V_2(k) \triangleq {s_2}^2(k), V_2(k+1) - V_2(k) < 0 \quad (13)$$

$${s_2}^2(k+1) - {s_2}^2(k) < 0 \rightarrow |s_2(k+1)| < |s_2(k)| \quad (14)$$

And $s_2(k+1)$ is one step ahead of $s_2(k)$:

$$\begin{cases} s_2(k+1) = \xi_2[\underline{x}(k), \boldsymbol{\phi}] + \frac{3T}{2} b_1 v_2(k-1) \\ \\ \xi_2[\underline{x}(k), \boldsymbol{\phi}] = i_2(k-1) + \frac{3T}{2}[a_{11} i_2(k-1) + \\ a_{12}\omega(k-1)] - \frac{T}{2}[a_{11} i_2(k-2) + a_{12}\omega(k-2) \\ +b_1 v_2(k-2)] - i_d(k) + \lambda_2[i_2(k-1) - i_d(k-1)] \end{cases} \quad (15)$$

Same as the followed procedure for obtaining the stability region for $v_1(k-1)$, $v_2(k-1)$ is calculated as shown in (12) to (17). Similar to part B in this section, the variables of these operators are also symbolic and converted to numerical values for digital implementation purposes. The two operators narrow the stability region, resulting in a robust torque controller.

$$\begin{cases} \frac{1}{min(b_1)} \frac{2}{3T} sup\big[- \xi_2[\underline{x}(k), \boldsymbol{\phi}] - |s_2(k)|\big]_{\boldsymbol{\phi}_U} \\ < v_2(k-1) < \frac{1}{max(b_1)} \frac{2}{3T} inf\big[- \xi_2[\underline{x}(k), \boldsymbol{\phi}] + |s_2(k)|\big]_{\boldsymbol{\phi}_U} \end{cases} \quad (16)$$

$$\begin{cases} v_2(k-1) = (1-\alpha_2)\Big[\frac{1}{max(b_1)} \frac{2}{3T} inf\big[- \xi_2[\underline{x}(k), \boldsymbol{\phi}] \\ +|s_2(k)|\big]_{\boldsymbol{\phi}_U}\Big] + \alpha_2\Big[\frac{1}{min(b_1)} \frac{2}{3T} sup\big[- \xi_2[\underline{x}(k), \boldsymbol{\phi}] \\ - |s_2(k)|\big]_{\boldsymbol{\phi}_U}\Big], 0 \le \alpha_2 \le 1 \end{cases} \quad (17)$$

Remark 1. $\tau_d(k)$ is not measurable as it belongs to the next loop of calculation and is assumed to be equal to $\tau_d(k-1)$.

Remark 2. By applying a simultaneous differentiation and lagged integration on the angular velocity, the angular acceleration of the output shaft is obtained. This leads to an estimation of the term $\tau_d(k-1)$, using (2). The dynamic effect of the operator is assumed to be negligible, since the operator has fast dynamics and the control system is desired to be simpler.

Remark 3. The sampling time is higher than twice the value of the maximum frequency of desired trajectories, which is critical for preserving the stability of the control system.

IV. The Proposed ADDR Method

The main objective of the ADDR method is to have a stabilized and precise position control. Although the SMC method is used to control the position and is inherently robust, it is unable to reject disturbance when it is unpredictable. Knowing that the presence of deteriorating vibration or unknown uncertainty cause an inevitable loss of precision, two actuators (PMDC machines) for this application are needed to cooperate simultaneously. The main actuator controls the position, while the auxiliary machine is responsible for disturbance rejection and active variable damping. Comparing the formation of $s_1(k)$ and $s_2(k)$, presented in section III, it can be seen that $s_2(k)$ is two steps ahead of $s_1(k)$, in terms of their consisting variables. This is caused due to the different orders of the differential equations between 'voltage and current', and 'voltage and position', which are first-order and third-order in PMDC motors, respectively. The validity of this claim can be proven by solving the Rosenbrock form of (2) in the frequency domain. Thus, torque control has a faster and superior performance for disturbance rejection and active damping, compared to position control. The ADDR method is a combination of the two previously mentioned algorithms, and switching occurs between the two based on the zero-slope detection of the angular position.

A. Disturbance Rejection

In order to have a smooth and stable position control in the presence of a deteriorating vibration of the structure, the following current should be tracked by the auxiliary actuator for disturbance rejection. The required current is not an independent variable and should be determined based on the resulted disturbance in the system, which depends on the angular acceleration, the position of the pendulum, and the total exerted torque on the output shaft. First, the exerted disturbance is estimated by deploying a model-based observer presented in (18), derived from (1), and secondly, the disturbance is rejected by the auxiliary actuator according to the estimated value. This required current($i_{d_{DR}}$) is a part of the ADDR method, tracked by the DTSMC-based controller developed in Section III and presented in (19).

$$\tau_d(k-1) = J_{eq}\ddot{\theta}(k-1) - \tau_t(k-1) + mgl sin[\theta(k-1)] \quad (18)$$

$$i_{d_{DR}}(k-1) = -\frac{\tau_d(k-1)}{K_t} \quad (19)$$

B. Active Variable Damping

To reduce the oscillations at peak values of any desired trajectory or to maintain a position stably, a damping logic is needed. Peak values are the positions where the angular velocity hovers around zero instantaneously. The auxiliary actuator is used to implement the damping algorithm for such motion, and it utilizes DTSMC to track the desired proposed current. To reach zero velocity, and assumed to have a constant acceleration at the peak points of trajectories the required torque is derived according to (20):

$$i_{d_{AVD}}(k-1) = -\frac{(m\omega^2(k-1)l^3)}{2K_t\Delta\theta} sign[\omega(k-1)] \quad (20)$$

where $i_{d_{AVD}}$ is the desired c urrent and $\Delta\theta$ is the estimated distance for the implementation of the active damping algorithm.

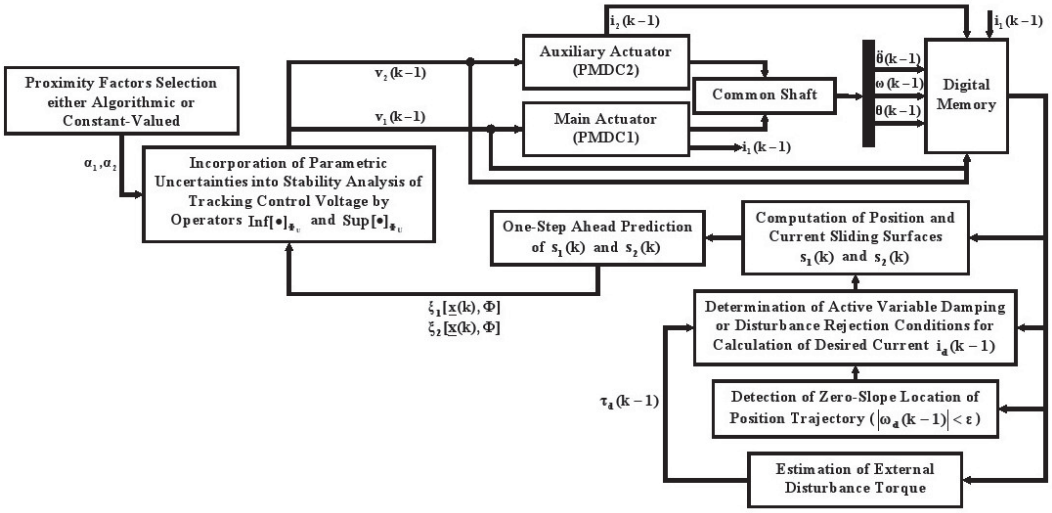

Fig. 3 General block diagram of DTSMC-based ADDR method

Conclusively, the desired current to be tracked by the DTSMC-based torque controller of the auxiliary actuator, is resulted according to (21) and (22):

$$i_d(k-1) \triangleq \eta(k-1) i_{d_{AVD}} + [1-\eta(k-1)] i_{d_{DR}} \tag{21}$$

$$\eta(k-1) = \begin{cases} 1 & |\omega_d(k-1)| < \varepsilon \\ 0 & |\omega_d(k-1)| > \varepsilon \end{cases} \tag{22}$$

where $\eta(k)$ is the switching signal, ω_d is the desired rotational velocity, derived by differentiating θ_d, and ε is a prescribed threshold of angular velocity value for zero-slope detection, according to which the switching occurs to dissipate energy from the system mounted on the moving/vibrating structure. This is done to obtain minimum rotary system oscillations at the peak points. $\Delta\theta$ is also calculated based on the switching point, which is in the vicinity of rest/peak points so that the controlled system gains an initial velocity before the active variable damping is incorporated in position stabilization.

Remark 4. The proposed torque controller requires the value of $i_d(k)$, which cannot be computed one step ahead, thus the desired current of the next step is assumed to be equal to the present desired value of the current i. e. , $[i_d(k) \sim= i_d(k-1)]$. The schematic of the proposed ADDR method is illustrated in Fig. 3.

V. Experimental Validation of the Method

A. Description of the ADDR Mechanical and Electrical System

To examine the ADDR technology experimentally, a dual-actuated rotary system is designed which consists of two PMDC machines, a tachometer, and an output shaft carrying a pendulum. These components are connected via 4 P13XL037F pulleys and a 94XL timing belt. A load is carried by the pendulum and the whole system is mounted on a linear actuator. The linear actuator tracks a vibrational motion to simulate oscillation-transmitting structures. The two PMDC machines are assumed to be identical and are of type ElectroCraft DP20. A tachometer and a two-channel optical encoder with a resolution of 500 pulse/rev are mechanically attached to the output shaft. Each PMDC is independently driven by a BTS7960B where the armature current is measured by a conventional hall-effect sensor. For ease of data acquisition and existence of multiple analog feedback signals, two digitally addressed analog multiplexers (SN741S157N) are utilized, and each connects eight lines to the microprocessor ADC ports. The microprocessor is ATMEGA2560 with an 8KB SRAM, 4KB EEPROM, and 16MHz CPU clock. Fig. 5 represents a picture of the assembled dual-actuated rotary system.

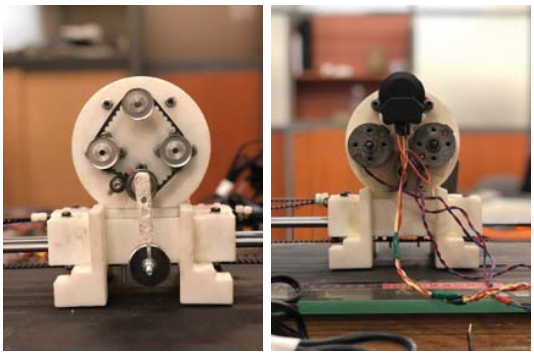

(a) (b)

Fig. 4 The dual-actuated rotary system and the linear actuator (a) front view of the rotary system, (b) back view of the rotary system

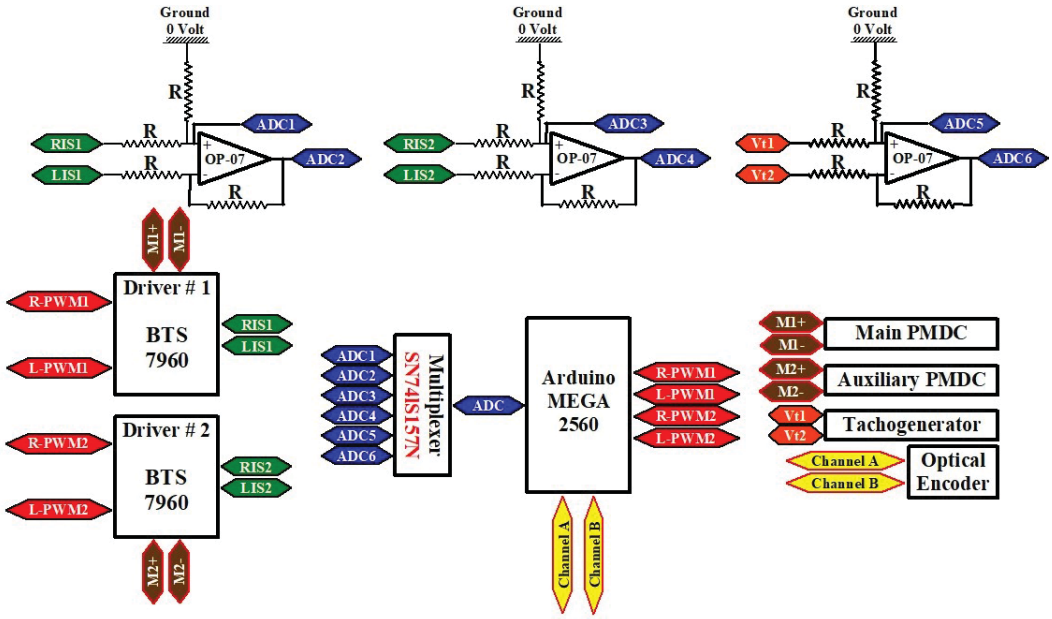

Fig. 5 The schematic of the driving circuit

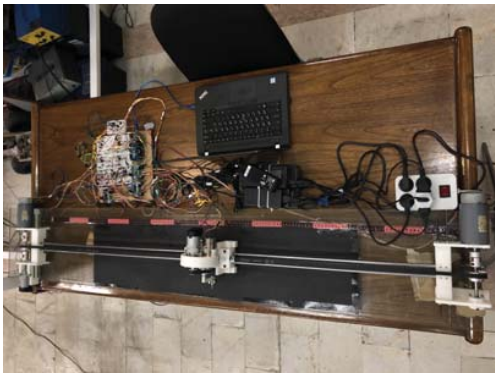

(a)

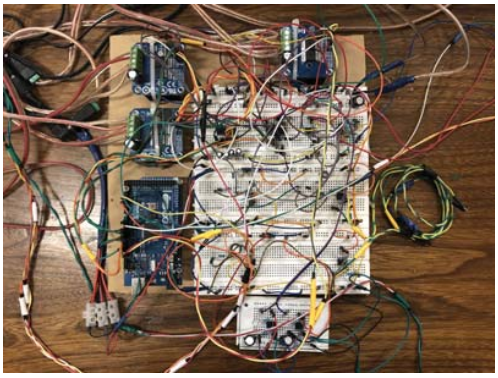

(b)

Fig. 6 (a) The general configuration of the experimental setup, (b) The electrical solderless circuitry of the ADDR machine

B. Performed Tests and Discussion

To assess the proposed ADDR technology, a harmonic and a piecewise step function are selected as the desired trajectories with an amplitude of A_1 and angular frequency of Ψ_1.

$$\begin{cases} Harmonic : \theta_d = A_1 sin(\Psi_1 t)[Deg] \\ Piecewisestep : \theta_d = A_1 sign[sin(\Psi_1 t)][Deg] \end{cases}$$

In both cases, the dual-actuated rotary system is being carried and vibrated by the attached cart beneath, which induces detrimental oscillations on the system. The linear actuator tracks the following motion, with amplitudes of A_2 and A_3, and angular frequencies of $10\Psi_1$ and Ψ_2.

$$x_l = A_2 sin(\Psi_2 t) + A_3 sin(10\Psi_1 t)[m]$$

The position of the linear actuator was experimentally obtained and its acceleration was obtained using the low-pass filtered differentiation method [15]. These two graphs and the estimation of disturbance which was acquired according to (18) are presented in Fig. 7.

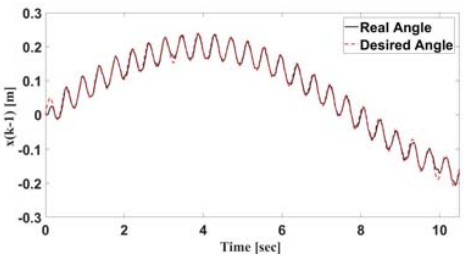

(a)

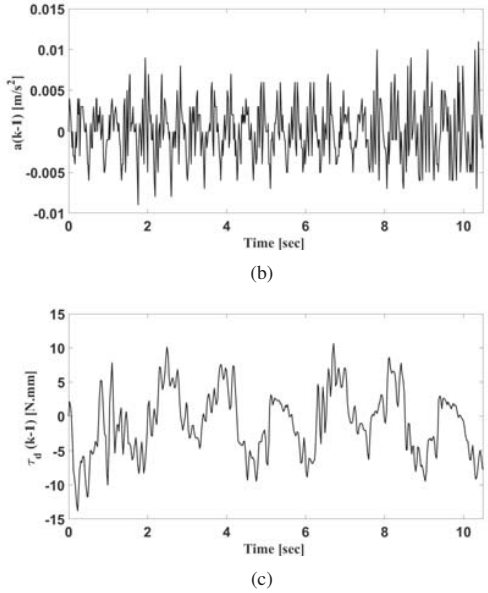

Fig. 7 (a) The position of the linear actuator, (b) The resulted acceleration of the linear actuator on the rotary system, (c) The estimation of disturbance

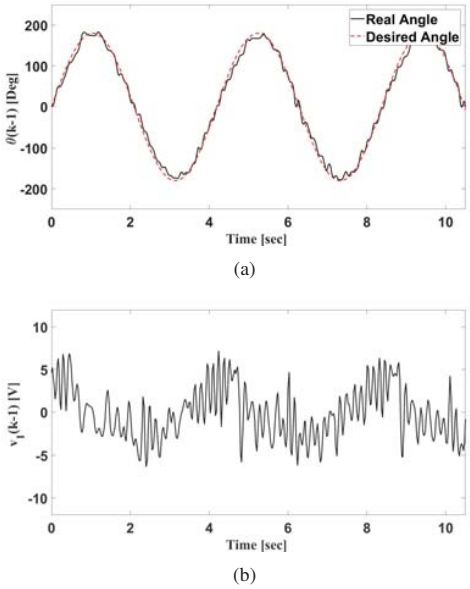

Fig. 8 (a) The performance of the position control scheme without additional assistance of the proposed ADDR, (b) Input voltage of the position controller

C. Test Steps

To evaluate the efficiency of the proposed ADDR technology, a comparison between the two techniques is arranged. In the first technique, the two actuators become unified and control the position, while the disturbance is included in their control algorithm. Whereas in the proposed ADDR technology, the auxiliary actuator is responsible for disturbance rejection using a torque controller, and the main actuator solely controls the position without accounting for the disturbance. For this purpose, the following test steps were proposed and conducted.

1) Position tracking of the desired harmonic trajectory, using position control
2) Position tracking of the harmonic desired trajectory with the assistance of the ADDR technology
3) Position tracking of the desired piecewise-step trajectory, using position control
4) Position tracking of the desired piecewise-step with the assistance of the trajectory ADDR technology

Step 1

The DTSMC- based position controller developed in III.C is implemented on the experimental setup. The utilized actuators work as a unified system with the input voltage obtained from 8. The performance of this position control method and the input voltage are illustrated in Fig. 8. This test is done without applying the proposed ADDR method in this paper, to show the performance of the controller without additional assistance of vibration isolation.

Step 2

To enhance the precision and quality of the controlled position, the main actuator is in charge of position control using DTSMC and the auxiliary actuator rejects disturbance, and damps the oscillations using the ADDR scheme presented in sectionIV. The obtained results are depicted in Fig. 9.

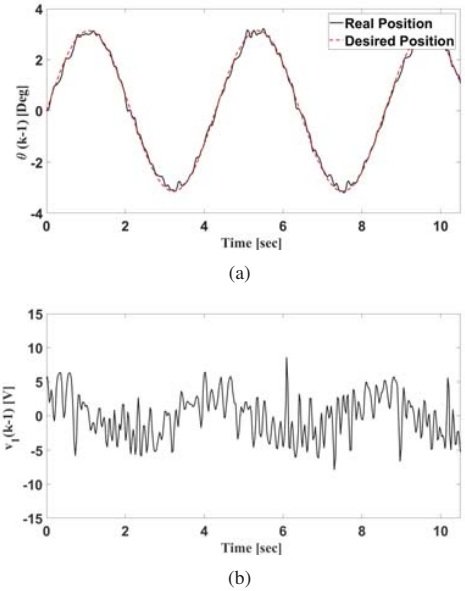

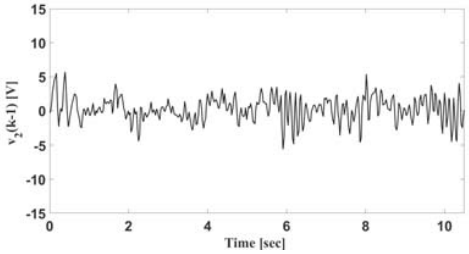

(c)

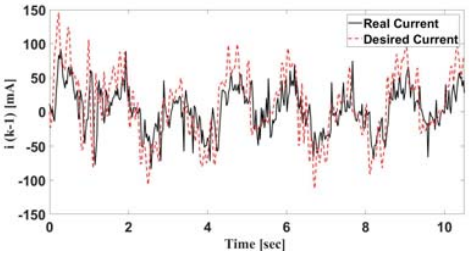

(d)

Fig. 9 (a) The performance of the ADDR technology for the harmonic sinusoidal trajectory, (b) Input voltage of the main actuator controlling the position, (c) Input voltage of the auxiliary actuator, (d) The performance of the auxiliary actuator following the desired current trend

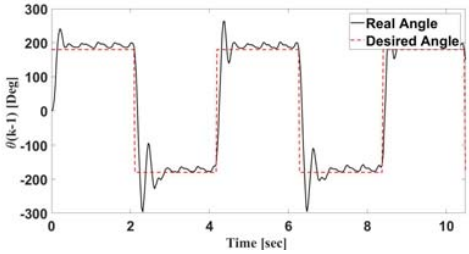

(a)

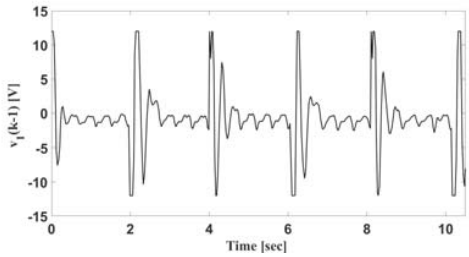

(b)

Fig. 11 (a) The performance of the position control scheme without additional assistance of the proposed ADDR method , (b) Input voltage of the position controller

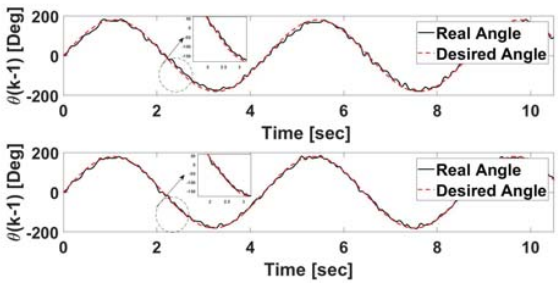

Fig. 10 A comparison between the performance of position control with and without applying the ADDR method shown by (a) and (b) respectively

Step 3

Same as the second step, position control using DTSMC was implemented on the experimental setup, but tracking a piecewise step trajectory is aimed at this time. The two utilized actuators work with the same input voltage simultaneously. The performance of this position control method is shown in Fig. 11. This test is done without applying the proposed ADDR scheme in this paper. As can be seen, the vibration of the base, on which the system is mounted, creates a challenging task for the position controller. The overshoot of the pendulum is increased and its ability to hold its position is declined.

Step 4

Similar to step 2, to enhance the precision, quality, and stability of the controlled position of the pendulum in step 3, the main actuator is used for position control and the motion is stabilized by the auxiliary actuator which applies the ADDR method, the obtained results are shown in Fig. 12.

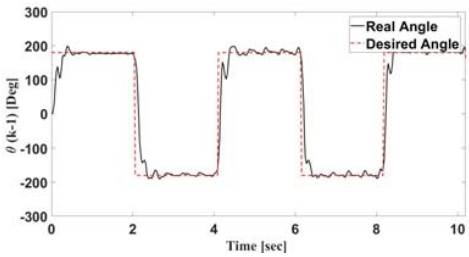

(a)

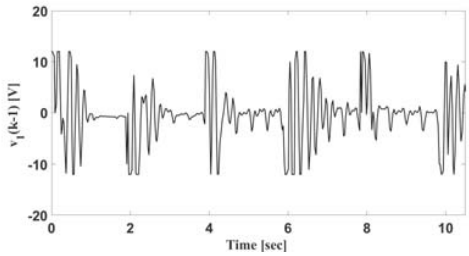

(b)

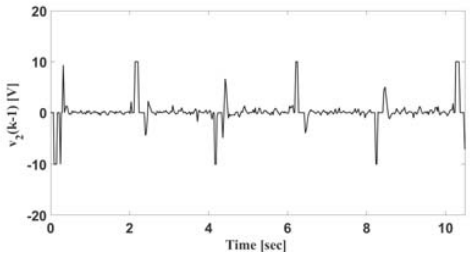

(c)

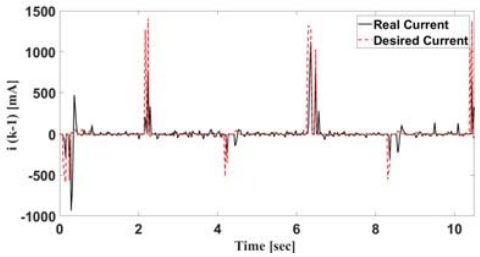

(d)

Fig. 12 (a) The performance of the position controller with the assistance of the ADDR technology, tracking the piecewise step trajectory, (b) Input voltage of the main actuator controlling the position, (c) Input voltage of the auxiliary actuator for disturbance rejection and active variable damping, (d) The performance of the auxiliary actuator following the desired current trend

D. Discussion

Sliding mode control is an algebraic controller and unlike adaptive or PID controllers, it does not require a differential equation to be solved. Therefore the controller is as fast as the open-loop system, and since a fast response is required for disturbance rejection and active variable damping, this control method has been adjusted.

The obtained results from the first two steps illustrate the superior performance of the second step compared to the first. With the help of ADDR technology, position tracking becomes smoother and more precise. The RMSE of the position tracking is improved by %27, from 10.3° degrees to 7.44° degrees. This happened due to successful disturbance rejection and active variable damping, and satisfactory performance of the DTSMC-based controllers. Moreover, by evaluating the acquired results from the last two steps, it is concluded that the oscillations are successfully damped and the disturbance is rejected in the last step when the algorithms are applied by the auxiliary actuator. Significant enhancement of the position tracking RMSE by %77 is resulted, improving from 12.60° degrees to 2.86° degrees.

VI. Conclusion

ADDR technology, applied to an auxiliary actuator, aiming for position tracking improvement was introduced and its superior performance compared to conventional vibration isolation methods was validated experimentally. This technology is applicable to any system demanding vibration isolation. In this practice, the method was implemented on a rotary system with a pendulum attached, mounted on a linear actuator simulating an oscillatory structure. The improved stability of the motion, offered by the proposed technology, was expected and obtained.

VII. Appendix A

TABLE I
PARAMETERS, VARIABLES, AND ACRONYMS USED IN THIS MANUSCRIPT

Parameters/ Variables/ Acronyms	Brief Description	Value
R_1	1st PMDC Rotor Winding Resistance (Ohm)	[2Ω]
R_2	2nd PMDC Rotor Winding Resistance (Ohm)	[2Ω]
R	Utilized Resistor in the Electrical Circuit (Ohm)	[6.8$k\Omega$]
L_1	1st PMDC Rotor Winding Inductance (Henry)	[4mH]
L_2	2st PMDC Rotor Winding Inductance (Henry)	[4mH]
K_{t1}	1st PMDC Torque Constant	[0.025$N.m/A$]
K_{t2}	2nd PMDC Torque Constant	[0.025$N.m/A$]
K_{e1}	1st PMDC Back-EMF Constant	[0.028$V.sec/rad$]
K_{e2}	2nd PMDC Back-EMF Constant	[0.028$V.sec/rad$]
J_{eq}	Effective Mass Moment of Inertia of the Rotation Axis ($kg.m^2$)	[0.0067$kg.m^2$]
m	Weight of the Pendulum (kg)	[0.05kg]
l	Length of the Pendulum (m)	[0.054m]
g	Gravitational Acceleration (m/s^2)	[9.81m/s^2]
$\theta(k)$	Angular Position of the Rotary System (rad)	–
$\ddot{\theta}(k)$	Angular Acceleration of the rotary System (rad/s^2)	–
τ_t	Total Torque of the Actuators (N.m)	–
T	Micro-controller loop time (second)	–
$i_1(k-1)$	Measured 1st PMDC Armature Current (A)	–
$i_2(k-1)$	Measured 2nd PMDC Armature Current (A)	–
$v_1(k-1)$	Measured 1st PMDC Armature Input Voltage (V)	–
$v_2(k-1)$	Measured 2nd PMDC Armature Input Voltage (V)	–
ω	Measured Actuator Rotational Velocity (rad/sec)	–
τ_t	Measured Disturbance of the System (N.m)	–
$V_1(k)$	Candidate Lyapunov Function for Position Tracking Control in Discrete Time	–
$V_2(k)$	Candidate Lyapunov Function for Torque Tracking Control in Discrete Time	–
$s_1(k)$	First Order Sliding Function for Position Control in Discrete Time	–
$s_2(k)$	First Order Sliding Function for Torque Control in Discrete Time	–
$i_{DR}(k)$	Desired Current for Disturbance Rejection (A)	–
$i_{AVD}(k)$	Desired Current for Active Variable Damping (A)	–
i_d	Desired Current (A)	–
θ_d	Desired Position (rad)	–
ϕ	The parameter Vector of the System	–
U	Uncertainty Space	–
$\alpha_1(k)$	Proximity Factor for Determination of $v_1(k)$	[Between 0 and +1]
$\alpha_2(k)$	Proximity Factor for Determination of $v_2(k)$	[Between 0 and +1]
λ_1	Sliding Surface Slope for Position Control	[Between -1 and +1]
λ_2	Sliding Surface Slope for Torque Control	[Between -1 and +1]
$\tilde{\theta}(k)$	Position Tracking Error of the Rotary System (rad)	
$\tilde{i}(k)$	Current Tracking Error (A)	–
$\underline{x}(k)$	State Vector	–
$\eta(k)$	Switching Signal	[Either 1 or 0]
A_1	1st Desired Amplitude	–
A_2	2nd Desired Amplitude	–
Ψ_1	1st Desired Angular Frequency	–
Ψ_2	2nd Desired Angular Frequency	–
ε	Reference Rotational Velocity Value for Zero-Slope Detection	–
RMSE	Root Mean Square Error	–
DTSMC	Discrete Time Sliding Mode Control	–

Declaration of Interest

The authors received no financial support for the research, authorship, and/or publication of this article.

References

[1] C. R. Fuller, S. J. Elliott, and P. A. Nelson, *Active vibration control*. Academic Press, 1996.
[2] R. E. Cunningham, "Steady-State Unbalance Response of a Three-Disk Flexible Rotor on Flexible, Damped Supports," J. Mech. Des., vol. 100, pp. 563–573, 1978.
[3] J. L. Nikolajsen and R. Holmes, "Investigation of Squeeze-Film Isolators for the Vibration Control of a Flexible Rotor," J. Mech. Eng. Sci., vol. 21, no. 4, pp. 247–252, 1979.
[4] T. Inoue, T. Sugai, and Y. Ishida, "Vibration Suppression of the Rotating Shaft using the Axial Control of the Repulsive Magnetic Bearing," J. Syst. Des. Dyn., vol. 4, no. 4, pp. 575–589, 2010.
[5] T. Inoue, H. Niimi, and Y. Ishida, "Vibration suppression of the rotor system using both a ball balancer and axial control of the repulsive magnetic bearing," J. Vib. Control, vol. 18, no. 4, 2010.
[6] A. Javed, T. Mizuno, M. Takasaki, I. Yuji, M. Hara, and D. Yamaguchi, "Lateral Vibration Suppression by Varying Stiffness Control in a Vertically Active Magnetic Suspension System," Actuators, vol. 7, 2018.
[7] C. Lusty and P. Keogh, "Active Vibration Control of a Flexible Rotor by Flexibly Mounted Internal-Stator Magnetic Actuators," IEEE/ASME Trans. Mechatronics, vol. 23, no. 6, 2018.
[8] C. . Knospe, R. . Hope, S. . Tamer, and S. . Fedigan, "Robustness of Adaptive Unbalance Control of Rotors with Magnetic Bearings," J. Vib. Control, vol. 2, no. 1, 1996.
[9] S. Li, J. Yang, W.-H. Chen, and X. Chen, Disturbance Observer-Based Control: Methods and Applications. CRC Press, 2016.
[10] W. A. S. P. Abeysiriwardhana and A. M. H. S. Abeykoon, "Simulation of active vibration suppression using internal motor sensing," in 7th International Conference on Information and Automation for Sustainability, 2014.
[11] S. Khan and A. Sabanovic, "Discrete-time Sliding Mode Control of High Precision Linear Drive using Frictional Model," in 9th IEEE International Workshop on Advanced Motion Control, 2006.
[12] A. Jafari Koshkouei and A. S.I.Zinober, "Discrete-Time Sliding Mode Control Design," IFAC Proc. Vol., vol. 29, no. 1, pp. 3350–3355, 1996.
[13] P.Sen, Principles of Electric Machines and Power Electronics, 3rd ed. John Wiley & Sons, 2013.
[14] E. Hairer, S. P. Norsett, and G. Wanner, Solving Ordinary Differential Equations. Springer, 1987.
[15] M. Athans, Modern Control Theory. Center for Advanced Engineering Study, Massachusetts Institute of Technology, 1974.

Kamand Bagherian received her B.Sc. degree from K. N. Toosi University of Technology, Tehran, Iran. Her research interests include nonlinear control, state/parameter estimation, and mechatronics.

Nariman Niknejad received his B.Sc. degree from K. N. Toosi University of Technology, Tehran, Iran. His research interests include nonlinear control, state/parameter estimation, and mechatronics.